Electron Affinity and Gas-Phase Electron Transfer Kinetics of (η^4-Butadiene)iron Tricarbonyl

Glen W. Dillow and Paul Kebarle*

Contribution from the Department of Chemistry, University of Alberta, Edmonton, Alberta, Canada T6G 2G2. *Received September 6, 1991*

Abstract: Pulsed high pressure mass spectrometry (PHPMS) was used to determine the thermochemistry of electron capture by (η^4-butadiene)iron tricarbonyl in the gas phase. The enthalpy ($\approx$-EA) and entropy for this process are -21.1 ± 1.0 kcal mol^{-1} and $+10 \pm 3$ cal K^{-1} mol^{-1}, respectively. The unusually large entropy change during electron capture is consistent with rupture of a Fe–alkene bond leading to increased internal freedom in the anion, as expected for the process: η^4-BdFe(CO)$_3$ + e = η^2-BdFe(CO)$_3^{\bullet-}$. The reaction rates of the electron transfer reactions, η^2-BdFe(CO)$_3^{\bullet-}$ + B = η^4-BdFe(CO)$_3$ + B$^{\bullet-}$, where B's are nitrobenzenes, were determined. The rate constants were found to increase with increasing reaction exoergicities and approached collision rates for exothermicities of $\sim$20 kcal mol^{-1}. Such rate dependence is consistent with a large geometry change as expected between η^2-BdFe(CO)$_3^{\bullet-}$ and η^4-BdFe(CO)$_3$. In competition with electron transfer, the molecular anion also undergoes unimolecular elimination of CO: η^2-BdFe(CO)$_3^{\bullet-}$ = η^4-BdFe(CO)$_2^{\bullet-}$ + CO. The Arrhenius activation energy for this process was measured and found to be E_A = 19.9 kcal mol^{-1}. By adding CO gas to the reaction system, the equilibrium of the elimination reaction was also determined, leading to ΔH = 20 kcal mol^{-1} and $\Delta S°$ = 28.3 cal K^{-1} mol^{-1}. Several novel ligand displacement reactions involving η^4-BdFe(CO)$_2^{\bullet-}$ with substituted nitrobenzenes were identified.

Introduction

Over the last 2 decades a considerable body of knowledge has been accumulated on the gas-phase negative ion chemistry of organometallic molecules.[1-3] Following early work on the formation and fragmentation of negative ions derived from organometallic species,[1,2] there is now a growing interest in the ion–molecule reactions of organometallic negative ions with organic and inorganic molecules.[2,3] It is becoming increasingly evident that, as with gas-phase ion–molecule studies involving organic positive and negative ions, these investigations are highly useful in defining the fundamental chemical reactivity of ionic species since complicating solvation and ion-pairing phenomena are completely absent. Despite the recent growth in this area of chemistry, however, the body of supporting thermochemical data covering organometallic negative ions is still remarkably limited.[3] This lack of information is particularly noticeable in the area of electron affinities (EAs), even though it is the EA of a molecule that provides direct information on the energy of the lowest unoccupied molecular orbital and is a major determinant of the basicity and nucleophilicity of the corresponding anion.[4]

In accordance with the 18-electron rule for organometallic species,[5] the majority of stable organometallic molecules possess a full valence shell and do not undergo resonance electron capture to yield stable anions because this would entail addition of an electron to an antibonding orbital. Molecules of this type may interact with electrons, reaction 1, to form transient anions which

$$ML_n + e^- \rightarrow [ML_n^{\bullet-*}] \rightarrow ML_n + e^- \quad (1)$$

decompose back to the molecule and a free electron because the molecule has a "negative EA"; i.e., the anion state lies at a higher energy than that of the neutral molecule plus a free electron.[6] Electron transmission spectroscopy has been used to determine the "negative EA" of a number of such organometallic molecules.[7]

Stable negative ions may be formed from 18-electron organometallic molecules by dissociative electron capture, reaction 2,

$$ML_n + e^- \rightarrow ML_{n-1}^{\bullet-} + L \quad (2)$$

where a stable negative ion is formed, only after the expulsion of a ligand molecule such as CO.[1-3] In cases where L is a two-electron donor, this leads to a 17-electron anion in which the electron occupies a bonding orbital and the 18-electron rule is not violated. Although this is the most common mechanism for negative ion formation from organometallic compounds, few EAs for ML_{n-1} fragments have been determined. EAs for the iron and nickel carbonyls, Fe(CO)$_{1-4}$ and Ni(CO)$_{1-3}$, have been determined by laser photodetachment of electrons from the corresponding anions.[8] More recently, the EAs of the oxo-chromium carbonyl species, Cr(CO)$_3$O$_2$ and Cr(CO)$_3$O, have been obtained from ion cyclotron resonance bracketing experiments.[9] In some cases, as with Mn(CO)$_5$ and Re(CO)$_5$, it has been possible to derive EAs from experimentally measured acidities and bond dissociation energies.[10]

In a recent communication[11] we reported the free energy change ($\approx$-EA) for electron capture by (η^4-butadiene)iron tricarbonyl, η^4-BdFe(CO)$_3$, which was determined by pulsed high pressure mass spectrometry (PHPMS). The EAs of $\approx$200 organic molecules have been measured recently by PHPMS, which has been demonstrated to be the method of choice for determining the EAs of molecules which attach electrons reversibly.[12,13] As an 18-electron molecule, η^4-BdFe(CO)$_3$ is unusual in that it undergoes "non-dissociative" electron capture[14-16] where an internal Fe–alkene bond is ruptured, but no ligand is eliminated because the butadiene remains coordinated to the iron atom through the second C=C double bond, reaction 3. Although this reaction can be

(1) Dillard, J. G. *Chem. Rev.* **1973**, *73*, 589.
(2) Gregor, I. K.; Guilhaus, M. *Mass Spectrom. Rev.* **1984**, *3*, 39.
(3) Squires, R. R. *Chem. Rev.* **1987**, *87*, 623.
(4) (a) Janousek, B. K.; Brauman, J. I. In *Gas Phase Ion Chemistry*; Bowers, M. T., Ed.; Academic Press: New York, 1979. (b) Bartmess, J. E.; McIver, R. T., Jr. In ref 4a.
(5) (a) Collman, J. P.; Hegedus, L. S.; Norton, J. R.; Finke, R. G. *Principles and Applications of Organotransition Metal Chemistry*; University Science Books: Mill Valley, CA, 1987. (b) Lukehart, C. M. *Fundamental Transition Metal Organometallic Chemistry*; Brooks/Cole Publishing Co.: Monterey, CA, 1987.
(6) Jordan, K. D.; Burrow, P. D. *Acc. Chem. Res.* **1978**, *11*, 341.
(7) (a) Giordan, J. C.; Moore, J. H.; Tossell, J. A.; Weber, J. *J. Am. Chem. Soc.* **1983**, *105*, 3431. (b) Burrow, P. D.; Guerra, M.; Jordan, K. D. *Chem. Phys. Lett.* **1985**, *118*, 328. (c) Modelli, A.; Distefano, G.; Guerra, M.; Jones, D. *J. Am. Chem. Soc.* **1987**, *109*, 4440. (d) Guerra, M.; Jones, D.; Distefano, G.; Foffani, A.; Modelli, A. *J. Am. Chem. Soc.* **1988**, *110*, 375.
(8) (a) Engelking, P. C.; Lineberger, W. C. *J. Am. Chem. Soc.* **1979**, *101*, 5569. (b) Stevens, A. E.; Feigerle, C. S.; Lineberger, W. C. *J. Am. Chem. Soc.* **1982**, *104*, 5026.
(9) Bricker, D. L.; Russell, D. H. *J. Am. Chem. Soc.* **1987**, *109*, 3910.
(10) Meckstroth, W. K.; Ridge, D. P. *J. Am. Chem. Soc.* **1985**, *107*, 2281.
(11) Dillow, G. W.; Nicol, G.; Kebarle, P. *J. Am. Chem. Soc.* **1989**, *111*, 5465.
(12) (a) Kebarle, P.; Chowdhury, S. *Chem. Rev.* **1987**, *87*, 513. (b) Kebarle, P. In *Techniques of Chemistry*; Saunders, W. H., Farrar, J. M., Eds.; Wiley Interscience: New York, 1988.
(13) (a) Paul, G.; Kebarle, P. *J. Am. Chem. Soc.* **1989**, *111*, 464. (b) Chowdhury, S.; Kishi, H.; Dillow, G. W.; Kebarle, P. *Can. J. Chem.* **1989**, *67*, 603. (c) Dillow, G. W.; Kebarle, P. *J. Am. Chem. Soc.* **1989**, *111*, 5592.
(14) Krusic, P. J.; San Fillipo, J., Jr. *J. Am. Chem. Soc* **1982**, *104*, 2645.
(15) Blake, M. R.; Garnett, J. L.; Gregor, I. K.; Wild, S. B. *J. Chem. Soc., Chem. Commun.* **1979**, 496.
(16) McDonald, R. N.; Schell, P. L.; Chowdhury, A. K. *J. Am. Chem. Soc.* **1985**, *107*, 5578.

0002-7863/92/1514-5742$03.00/0

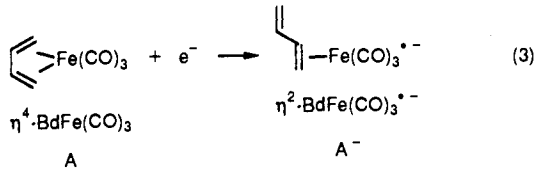

(3)

viewed as a dissociative electron capture process, it is reversible because the detached "ligand" remains attached to the anion, and, hence, electron transfer equilibria with other electron acceptor molecules may be achieved and measured by PHPMS. In this paper, we report the results of a more extensive series of PHPMS measurements involving electron capture by A. The enthalpy (=−EA) and entropy of electron capture by A were measured, along with the kinetics of electron transfer from the A^- to selected organic molecules, B. Also, the energetics of unimolecular CO elimination from the molecular anion were determined and some novel reactions of the resultant anion with aromatic molecules were identified.

Experimental Section

The gas-phase equilibria and kinetic measurements were performed with a pulsed electron high pressure mass spectrometer (PHPMS) which has been described previously.[12] The experimental procedures were essentially the same as described previously also.[12,13] Briefly, reaction mixtures in the ion source typically consisted of methane at 6 Torr pressure containing milliTorr quantities of η^4-BdFe(CO)$_3$ (A) and substituted-nitrobenzene reference compounds (B). Ion chemistry was initiated by directing a 10–200-μs pulse of 2-keV electrons into the ion source. The primary ionization of CH_4 by these electrons leads to secondary electrons which are thermalized by further collisions. Capture of these electrons by A and B leads to $A^{\bullet-}$ and $B^{\bullet-}$ as well as other product ions. Diffusion of the ions to the walls of the ion source is slow because of the relatively high ion source pressure used. The resulting relatively long lifetime of the ions allows ion–molecule equilibria to establish. Some of the ions come to the vicinity of the ion exit slit and are carried out into the vacuum of the ion acceleration and mass analysis region.

The temporal behavior of the ions was determined by monitoring the ion intensities for 10–20 ms after each pulse with a multichannel analyzer. In previous PHPMS studies of electron transfer equilibria, reaction times of ≈2 ms were typical, but longer reaction times were necessary in this study owing to the unusually slow electron transfer kinetics. To measure the electron transfer equilibrium (eq 4), the intensities of the

$$A^{\bullet-} + B = A + B^{\bullet-} \tag{4}$$

ions $A^{\bullet-}$ and $B^{\bullet-}$, $I(A^{\bullet-})$ and $I(B^{\bullet-})$, were determined at long reaction times, where the intensity ratio had become constant. This intensity ratio was then used in eq 5 for the evaluation of the equilibrium constant K_4.

$$K_4 = \frac{[B^{\bullet-}][A]}{[A^{\bullet-}][B]} = \frac{I(B^{\bullet-})[A]}{I(A^{\bullet-})[B]} \tag{5}$$

Equilibrium measurements were made over a range of temperatures enabling the electron transfer enthalpy and entropy to be determined from a van't Hoff plot of ln K_4 versus $1000/T$ (K).

As will become evident from the Results and Discussion section, large geometry differences exist between η^4-BdFe(CO)$_3$ and the radical anion since that species corresponds to η^2-BdFe(CO$_3$)$^{\bullet-}$. Because of the large geometry change, the kinetics of electron transfer in reaction 4, where η^4-BdFe(CO)$_3$ is either A or B, can be very slow,[12a] particularly in the endoergic direction of equilibrium 4. To speed up the rates and observe equilibria, the concentrations of the neutrals A and B were selected both to be relatively very high, and the concentration of the neutral reactant in the endoergic direction was orders of magnitude larger than the concentration of the neutral reactant in the exoergic direction. This procedure was used also in earlier PHPMS work.[12]

The rate constant for the electron transfer 4, where $A^{\bullet-}$ was BdFe(CO)$_3^{\bullet-}$ and B were compounds with known high electron affinities, was determined in separate experiments where, because of a special choice of reactants and reactant concentrations, the kinetic stage where $A^{\bullet-}$ was converted to $B^{\bullet-}$ was long and the plot ln $I(A^{\bullet-})$ versus time was linear. The slope of such plots provides the pseudo-first-order rate constant $\nu_4 = k_4[B]$. Plots of ν_4 versus [B], the concentration of B, led to straight lines whose slope yielded the rate constant k_4.

η^4-BdFe(CO)$_3$ was obtained from Strem Chemicals and used without further purification. Refrigeration of the sample between experiments was sufficient to prevent aerial oxidation of this compound over the period of this study. The substituted nitrobenzenes used in the electron transfer measurements were obtained from Aldrich Chemical Co. and were used without further purification but were purged with nitrogen prior to use.

In order to avoid thermal decomposition of the η^4-BdFe(CO)$_3$ in the gas handling manifold, the manifold temperature was limited to 70 °C. No evidence of thermal decomposition or of reactions between η^4-BdFe(CO)$_3$ and the nitrobenzenes within the manifold was observed at this temperature. However, this did place restrictions on the volatility of the compounds that could be used, and, hence, only liquid nitrobenzenes were included in this study.

Stringent efforts to exclude oxygen from the reaction system were necessary in order to obtain reliable and reproducible electron transfer equilibrium constants because $A^{\bullet-}$ reacts with O_2[17] at a rate comparable to the rate of electron transfer to the nitrobenzenes used in the equilibrium measurements.

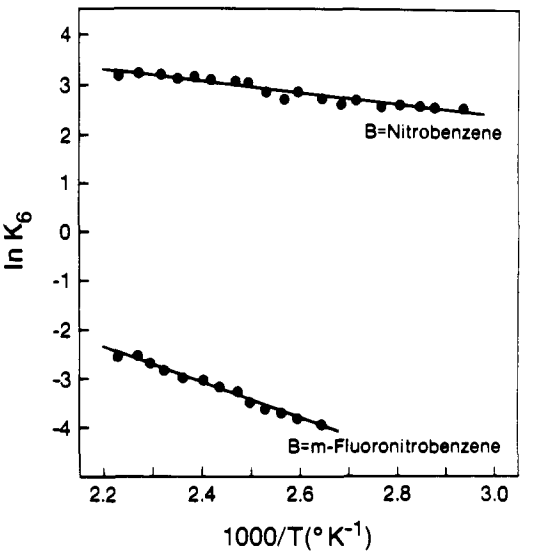

Figure 1. van't Hoff plots of equilibria 6: $B^{\bullet-} + \eta^4$-BdFe(CO)$_3$ = B + η^2-BdFe(CO)$_3^{\bullet-}$, where B = nitrobenzene and *m*-fluoronitrobenzene.

Table I. Thermochemical Data[a] from Electron Transfer Equilibria (Eq 6): η^4-BdFe(CO)$_3$ + $B^{\bullet-}$ = η^2-BdFe(CO)$_3^{\bullet-}$ + B

B	$\Delta H°_6$	$\Delta S°_6$	$\Delta H°_a$-(B)	$\Delta S°_a$-(B)	$\Delta H°_a$-(A)	$\Delta S°_a$-(A)
nitrobenzene	2.3	11.6	−23.2	−1.0	−20.9	+10.6
m-fluoronitrobenzene	7.1	11.0	−28.4	−1.7	−21.3	+9.3

[a] Enthalpies given in kcal/mol, entropies in cal deg^{-1} mol^{-1}. ΔH_a and ΔS_a are the energies for electron attachment; see eq 4. Literature values[13b,17] were used for $\Delta H°_a$(B) and $\Delta S°_a$(B). The $\Delta H°_a$(A) and $\Delta S°_a$(A), where A = η^4-BdFe(CO)$_3$, were evaluated from $\Delta H°_6$ + $\Delta H°_a$(B) and $\Delta S°_6$ + $\Delta S°_a$(B), respectively. The stationary electron convention[12a] is used in the evaluation of $\Delta G°_a$, $\Delta H°_a$, and $\Delta S°_a$.

Results and Discussion

(a) Enthalpy and Entropy of Electron Capture by η^4-BdFe(CO)$_3$. The equilibrium constants for electron transfer equilibrium 6, K_6,

$$\eta^4\text{-BdFe(CO)}_3 + B^{\bullet-} = \eta^2\text{-BdFe(CO)}_3^{\bullet-} + B \tag{6}$$

$$B + e^- \rightarrow B^{\bullet-} \tag{7}$$

$$\eta^4\text{-BdFe(CO)}_3 + e^- \rightarrow \eta^2\text{-BdFe(CO)}_3^{\bullet-} \tag{3}$$

where B = nitrobenzene and *m*-fluoronitrobenzene, were measured over a range of temperatures using PHPMS. The results of these measurements are presented as van't Hoff plots of ln K_6 versus $1000/T$ (K) in Figure 1. From the van't Hoff plots, the enthalpy and entropy changes for the electron transfer, $\Delta H°_6$ and $\Delta S°_6$, were determined by the standard procedure from the slope and *y*-intercept, respectively. These values are given in Table I. The enthalpy $\Delta H°_a$ and entropy $\Delta S°_a$ values for electron attachment

(17) Wang, D.; Squires, R. R. *Organometallics* **1987**, *6*, 905.
(18) Chowdhury, S.; Heinis, T.; Grimsrud, E. P.; Kebarle, P. *J. Phys. Chem.* **1986**, *90*, 2747.

by η^4-BdFe(CO)$_3$, reaction 3, were obtained by combining the thermochemical values for equilibrium 6 and the electron attachment reaction 7; see Table I. Since the two sets of results are in good agreement with each other, they were combined to yield the following mean values:

$$-EA \approx \Delta H^\circ_3 = \Delta H^\circ_a(\eta^4\text{-BdFe(CO)}_3) = -21.1 \pm 1.0 \text{ kcal mol}^{-1}$$

$$\Delta S^\circ_3 = \Delta S^\circ_a(\eta^4\text{-BdFe(CO)}_3) = +10 \pm 3 \text{ cal K}^{-1} \text{ mol}^{-1}$$

These results show that while the electron affinity of η^4-BdFe(CO)$_3$ is appreciable, i.e., $\Delta H^\circ_a(\eta^4\text{-BdFe(CO)}_3) = 21.1$ kcal mol^{-1} = 0.92 eV, electron capture is further favored by the large positive entropy change which occurs during negative ion formation. Indeed, $\Delta S^\circ_a = +10$ cal K^{-1} mol^{-1} is one of the largest electron capture entropy changes ever measured.[12] Thus, even though the EA of *m*-fluoronitrobenzene is higher by 7.1 kcal/mol than that of η^4-BdFe(CO)$_3$, electron transfer equilibrium between the two molecules can still be achieved because the unusually high value of $\Delta S^\circ_a(\eta^4\text{-BdFe(CO)}_3)$ compensates for the 7.1-kcal mol^{-1} endothermicity.

At 150 °C, ΔG°_a for η^4-BdFe(CO)$_3$, which corresponds to the free energy change for electron attachment by this molecule, equals −25.3 kcal mol^{-1}. It is worthwhile to note that in previous work, such as the preliminary communication of this work,[11] the approximation that $EA \approx -\Delta G^\circ_a$ has often been used; it is seen here that even with this unusually large ΔS°_a, the approximation is inaccurate by only 4 kcal mol^{-1} = 0.17 eV at 150 °C.

Formation of a molecular negative ion from η^4-BdFe(CO)$_3$ in the gas phase has been observed previously under "chemical ionization" conditions in a conventional mass spectrometer[15] and in a flowing afterglow apparatus.[16,17] Significantly, this anion has also been generated in solution from η^4-BdFe(CO)$_3$ by electrochemical methods.[14,19] This was an important development because it allowed the anion to be characterized by conventional techniques. It was established that the one-electron reduction of η^4-BdFe(CO)$_3$ is reversible, and this is consistent with no loss of CO groups or the butadiene group but formation of a molecular radical anion. Krusic et al.[14] found that the ESR spectrum observed after reduction was a (not fully resolved) triplet of doublets as expected for the interactions of the unpaired electron with two equivalent and one nonequivalent hydrogen nuclei. This is strong evidence that the unpaired electron, located largely on the Fe, interacts with the three H atoms of one of the vinyl groups of butadiene; i.e., a reduction of the hapticity of the butadiene from η^4 to η^2 corresponding to η^2-BdFe(CO)$_3^{\bullet-}$ has occurred. η^2-BdFe(CO)$_3^{\bullet-}$ is formally a d^9 17-electron species in which the electron occupies the uppermost iron 3d orbital. From ESR results on matrix isolated Fe(CO)$_4^{\bullet-}$,[20] which is closely related to (alkene)Fe(CO)$_3^{\bullet-}$ anions, one may conclude that this orbital is predominantly $3d_{z^2}$ in character. The LUMO is antibonding in η^4-BdFe(CO)$_3$, in accordance with the 18-electron rule, but bonding in η^2-BdFe(CO)$_3$.[21]

In previous studies[11,16,17] of electron capture by η^4-BdFe(CO)$_3$ in the gas phase, it was assumed that the nature of the anion in the gas phase is the same as in solution, but this has not been confirmed experimentally to date. The large positive value of $\Delta S^\circ_a(\eta^4\text{-BdFe(CO)}_3)$ indicates that a substantial structural change occurs upon electron capture by η^4-BdFe(CO)$_3$, and is therefore consistent with decoordination of one of the butadiene alkene bonds as represented in reaction 3. A quantitative comparison of the measured ΔS°_a, ≈10 cal deg^{-1} mol^{-1}, with a ΔS°_a obtained from a detailed consideration of the changes of internal motions and evaluation of the resulting entropy changes on the basis of statistical mechanics is not possible because structural data for η^2-BdFe(CO)$_3^-$ are almost entirely lacking. Therefore, only a very qualitative account can be given.

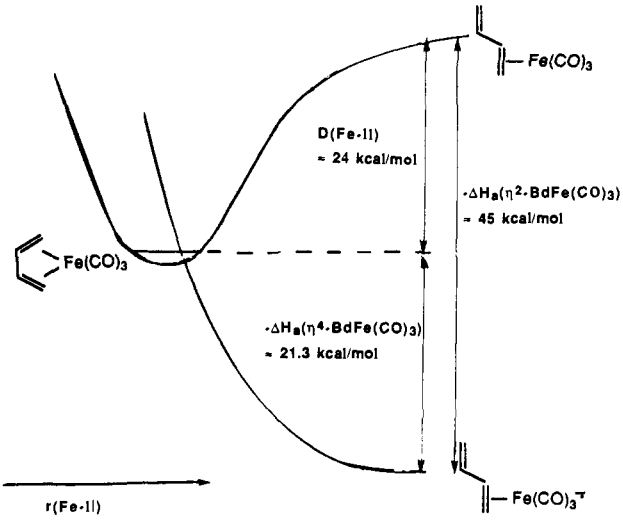

Figure 2. Schematic diagram for energy changes on electron capture by η^4-BdFe(CO)$_3$ and η^2-BdFe(CO)$_3$ and deduced electron attachment energy $\Delta H_a(\eta^2\text{-BdFe(CO)}_3) \approx -45$ kcal mol^{-1}. Horizontal axis corresponds to distance of second double bond of Bd to Fe atom.

The vibrational spectrum[22] of η^4-BdFe(CO)$_3$ includes some six vibrations whose frequencies are below 400 cm^{-1} (380, 360, 350, 133, 115, 102). In all of these, motions of the butadiene relative to the Fe(CO)$_3$ group dominate. It is exactly these vibrations, whose frequencies are already small and thus make large contributions to the entropy, that will be further softened by the conversion to η^2-BdFe(CO)$_3^{\bullet-}$. Thus, if we assume that each of these frequencies reduces to one-half on electron attachment, a $\Delta S^\circ \approx 7.8$ cal deg^{-1} mol^{-1} results.[23] In addition to this, a rotation of the vinyl group around the C–C bond in butadiene becomes possible in η^2-BdFe(CO)$_3^{\bullet-}$, replacing higher frequency motions in the decoordinated Bd. Approximating the bulk of the η^2-BdFe(CO)$_3^{\bullet-}$ as a rotor whose moment of inertia is infinitely larger than that of the vinyl group and assuming a barrier of 5 kcal/mol for the internal rotation, one obtains[23] an entropy gain of 5 cal deg^{-1} mol^{-1} and a combined total, $\Delta S^\circ_a \approx 13$ cal deg^{-1} mol^{-1}, which is close to the measured 10 cal deg^{-1} mol^{-1}.

The yield of negative ions due to electron capture of free electrons by η^4-BdFe(CO)$_3$, observed in the present work, was much higher than that for the nitrobenzenes. In the high pressure ion source most of the electrons have been thermalized, and a high negative ion yield is observed only when the electron capture cross section is largest for thermal electrons. Therefore, it is likely that the η^4-BdFe(CO)$_3$ electron capture cross section is at its maximum for thermal electrons. The potential energy curves involved in the electron capture process can then be represented by the diagram shown in Figure 2. The geometry parameter represented in the *x* axis involves mostly the distance between Fe and the vinyl group that becomes decoordinated in the radical anion. The average Fe–alkene bond dissociation energy in η^4-BdFe(CO)$_3$ has been measured to be 24 kcal mol^{-1} by microcalorimetric thermal decomposition methods.[24] A similar value, 23.1 kcal/mol, was obtained[24] for the Fe–C_2H_4 bond energy in (C_2H_4)Fe(CO)$_4$. On this basis, we have taken 24 kcal/mol to be equal to the energy to produce the singlet η^2-BdFe(CO)$_3$ from the η^4-BdFe(CO)$_3$; see Figure 2. However, it should be noted, as in the case[21] for Fe(CO)$_4$, the triplet state of η^2-BdFe(CO)$_3$ is likely to be somewhat more stable than the singlet state. Introducing the value $\Delta H_a[\eta^4\text{-BdFe(CO)}_3] = -21.3$ kcal/mol (see Figure 2), one obtains an estimate for the electron affinity of η^2-BdFe(CO)$_3$; $-\Delta H^\circ_a[\eta^2\text{-BdFe(CO)}_3] \approx 45$ kcal mol^{-1}. This value can be also taken

(19) El Murr, N.; Payne, J. D. *J. Chem. Soc., Chem. Commun.* **1985**, 162.
(20) (a) Breeze, P. A.; Burdett, J. K.; Turner, J. J. *Inorg. Chem.* **1981**, *20*, 3369. (b) Peake, B. M.; Symons, M. C. R.; Wyatt, J. L. *J. Chem. Soc., Dalton Trans.* **1983**, 1171.
(21) Albright, T. A.; Burdett, J. K.; Whangbo, M.-H. *Orbital Interactions in Chemistry*; Wiley-Interscience: New York, 1985; Chapters 18 and 19.
(22) Davidson, G. *Inorg. Chim. Acta* **1969**, *3*, 596.
(23) Benson, S. W. *Thermochemical Kinetics, 2nd ed.*; Wiley-Interscience: New York, 1976.
(24) Brown, D. L. S.; Connor, J. A.; Leung, M. L.; Paz-Andrade, M. I.; Skinner, H. A. *J. Organomet. Chem.* **1976**, *110*, 79.

Table II. Rate Constants[a] for Electron Transfer Reactions (Eq 8): η^2-BdFe(CO)$_3^{\bullet-}$ + B = η^4-BdFe(CO)$_3$ + B$^{\bullet-}$

B[b]	$\Delta H°_8$	$\Delta G°_8$	k_8
m-F-NB[c] (28.3; 26.0)	−7.3	−2.4	5×10^{-12}
m-CF_3-NB (32.4; 31.6)	−11.3	−8.0	4.3×10^{-11}
OCHO-NB (35.9; 34.6)	−14.8	−11.0	8.3×10^{-11}
3,5-bis-CF_3-NB (41.3; 40.2)	−20.2	−16.6	4.7×10^{-10} (150 °C)
3,5-bis-CF_3-NB (41.3, 40.2)	−20.2	−16.6	6.2×10^{-10} (117 °C)

[a] Rate constants in molecule^{-1} cm^3 s^{-1} at 150 °C. $\Delta H°_8$ and $\Delta G°_8$ in kcal/mol. These values were obtained with the expressions: $\Delta H°_8 = \Delta H°_a$(B) − $\Delta H°_a$(η^4-BdFe(CO)$_3$) and analogous expression for ΔG. The $\Delta H°_a$, $\Delta G°_a$ for B used[12a,13b] are given in parentheses beside each B. For η^4-BdFe(CO)$_3$, ΔH_a = −21.1 kcal/mol and $\Delta G°_a$ = −23.63 kcal/mol at 150 °C; see section a. [b] NB stands for nitrobenzene. [c] Rate constant from previous determination.[11]

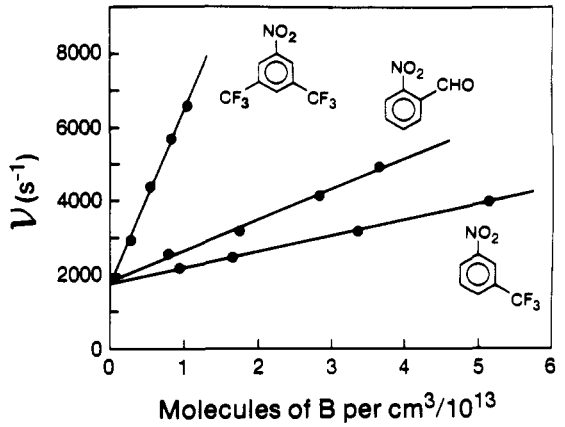

Figure 3. Plot of the reaction frequency (pseudo-first-order rate constant) for the decay of the η^2-BdFe(CO)$_3^{\bullet-}$ versus the concentration of B. Slope of straight lines provides rate constant k_8 for reaction 8: η^2-BdFe(CO)$_3^{\bullet-}$ + B = η^4-BdFe(CO)$_3$ + B$^{\bullet-}$.

to represent an upper limit for the activation energy barrier for electron transfer from η^2-BdFe(CO)$_3^-$ to species B like the nitrobenzenes, which on capture of electrons undergo only very small geometry changes; see next section.

(b) Electron Transfer Kinetics. Measurement of the electron transfer equilibria described in the preceding section was hampered to some extent by the slow rate of electron transfer between reactants. As a result of the slow electron transfer kinetics, side reactions such as reactions of η^2-BdFe(CO)$_3^{\bullet-}$ with oxygen[17] occurred sufficiently rapidly to interfere with the equilibria measurements unless unusual care was taken to exclude air from the reaction mixture. As reported previously,[11] the rate constant for electron transfer from η^2-BdFe(CO)$_3^{\bullet-}$ to *m*-fluoronitrobenzene was 5×10^{-12} cm^3 molecule^{-1} s^{-1}, which is only ≈0.25% of the collisional rate constant. Given that this reaction is exoergic by 2.4 kcal mol^{-1} and exothermic by 7.3 kcal mol^{-1}, and that even moderately exothermic electron transfer reactions generally proceed at virtually every collision,[12a] the efficiency of electron transfer reactions involving η^2-BdFe(CO)$_3^{\bullet-}$ is clearly unusually low. Cases of slow electron transfer kinetics have been encountered previously and associated with large geometry changes during the reaction.[25] The same cause is suggested by the diagram in Figure 2 for the present electron transfer reactions.

To further examine the slow electron transfer kinetics, the kinetics for reaction 8 involving electron transfer from η^2-BdFe(CO)$_3^{\bullet-}$ to several acceptor molecules having different electron affinities were measured at a reaction temperature of 150 °C. The electron acceptors used in these experiments, as well as their $-\Delta H°_a$ (kcal mol^{-1}) and $-\Delta G°_a$ (150 °C) (kcal mol^{-1}) values,[12a,13b] are given in Table II. Plots of the measured rate of decay of

$$\eta^2\text{-BdFe(CO)}_3^{\bullet-} + \text{B} \rightarrow \eta^4\text{-BdFe(CO)}_3 + \text{B}^{\bullet-} \qquad (8)$$

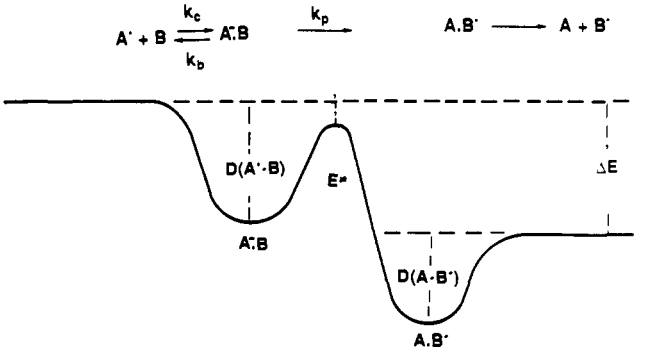

Figure 4. Potential energy diagram for gas-phase electron transfer with large internal barrier. Marcus theory cannot be applied when $D(A^-$–B) is very different from D(A–B$^-$).

η^2-BdFe(CO)$_3^{\bullet-}$ as a function of the concentration of B at 150 °C are shown in Figure 3. For each particular reaction mixture, the measured pseudo-first-order rate constant for decay of the η^2-BdFe(CO)$_3^{\bullet-}$, which will be called the reaction frequency of the ion, ν_i (s^{-1}), is described by the expression:

$$\nu_i = k_8[\text{B}] + \nu_d + k_{10} \qquad (9)$$

where k_8 is the rate constant for the bimolecular reaction 8, ν_d is the reaction frequency for ion loss by diffusion to the ion source walls,[12b] and k_{10} is the rate constant for the unimolecular decomposition of the ion which proceeds by CO elimination; see reaction 10 in section c.

According to eq 9, the slopes of the straight-line plots in Figure 3 correspond to k_8. The rate constant k_8 obtained in this manner are given in Table II together with the k_8 value for B = *m*-F–NB obtained in the earlier determination.[11]

The results demonstrate that k_8 is strongly dependent on the reaction exothermicity and exoergicity. Thus, $k_8 = 5 \times 10^{-12}$ molecule^{-1} cm^3 s^{-1} for $\Delta H°_8$ = −7.3, $\Delta G°_8$ = −2.4 kcal mol^{-1}, and hundred times higher, $k_8 = 4.7 \times 10^{-10}$ molecule^{-1} cm^3 s^{-1} for $\Delta H°_8$ = −20.2, $\Delta G°_8$ = −16.6 kcal mol^{-1}; see Table II. Even for this highest exothermicity, k_8 is still only one-fourth of the collision limit $k \approx 2 \times 10^{-9}$ molecule^{-1} cm^3 s^{-1}.

The temperature dependence of k_8 was examined for one case, B = 3,5-bis-CF_3-NB, the most exothermic reaction; see Table II. A decrease of temperature from 150 °C to 117 °C led to an increase of the rate constant from $k_8 = 4.7 \times 10^{-10}$ to 6.2×10^{-10} molecule^{-1} cm^3 s^{-1}. Such a negative temperature dependence is characteristic of ion–molecule reactions in which a substantial central barrier is present and the height of the barrier lies below the energy of the reactants;[25] see double well potential diagram, Figure 4.

The increase of the rate constants, at a given temperature, with increasing exothermicity and exoergicity of the reaction observed in Table II follows a pattern very similar to that observed in previous work from this laboratory[25] involving electron transfer from $SF_6^{\bullet-}$ to substituted nitrobenzenes B. In that case, a large geometry change between the ground-state structures of SF_6 and SF_6^- was expected, as is the case also for the present system. Theoretical predictions of the geometries of SF_6 and $SF_6^{\bullet-}$ were available,[26] while for the nitrobenzenes B and B$^{\bullet-}$ the geometry changes are expected to be small. It was therefore possible to estimate[25a] the barriers E^*, (see Figure 4) for the electron transfer:

$$SF_6^{\bullet-}\cdot\text{B} \rightarrow SF_6\cdot\text{B}^{\bullet-}$$

where B's were substituted nitrobenzenes leading to different exothermicities of the reaction.

Richardson,[27] on the basis of the same theoretical calculations[26] of the SF_6 and SF_6^- energies as a function of geometry, also obtained estimates for this barrier, with use of the established formalism[26] of the Marcus electron transfer theory.[28] The

(25) (a) Grimsrud, E. P.; Chowdhury, S.; Kebarle, P. *J. Chem. Phys.* **1985**, *83*, 1059. (b) Chowdhury, S.; Kebarle, P. *J. Chem. Phys.* **1986**, *85*, 4989.

(26) Hay, P. J. *J. Chem. Phys.* **1982**, *76*, 502.
(27) Richardson, D. E. *J. Phys. Chem.* **1986**, *90*, 3697.

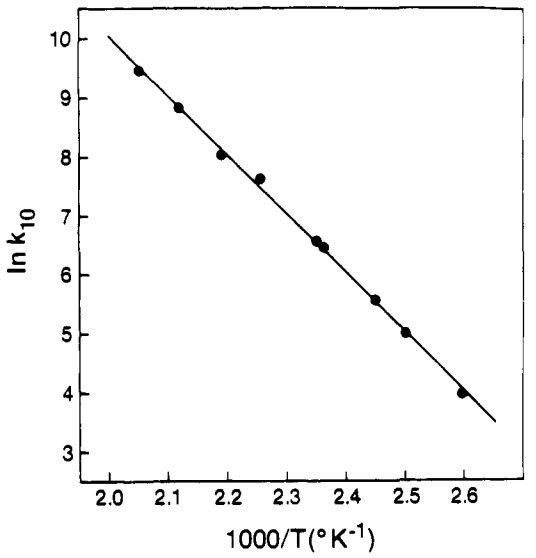

Figure 5. Arrhenius plot of rate constant k_{10} for the reaction η^2-BdFe-$(CO)_3^{\bullet-} \rightarrow \eta^4$-BdFe$(CO)_2^{\bullet-}$ + CO.

magnitudes of the barriers[25a,27] were very similar. However, a special difficulty regarding the barrier height in gas-phase electron transfer reaction exists. The reaction coordinate not only involves displacements due to different geometries of A, A^- and B, B^-, but also displacements connected with the type of intermolecular bonding in A^-–B and A–B^- which determine the well depths; see Figure 4. For SF_6 and nitrobenzenes, the bonding in the two complexes changes very considerably.[25b] It is likely that this will be also the case for the present reaction 8. When the two well depths are very different, the reaction coordinated depends in a complex manner on several vibrational modes, and the activation barrier cannot be evaluated with the Marcus equation[28,29] which includes ΔE, the exothermicity of the reaction. Dodd and Brauman[30a] have considered the difficulty posed by the different well depths and their lack of direct relationship to ΔE. These authors have provided a modified Marcus equation for the evaluation of an effective barrier, $E^{\ddagger}_{eff}$, which can be related to ΔE. The reaction systems considered were S_N2 reactions,[30a] and for these established assumptions are available regarding the nature of the transition state. Therefore, the evaluation of the sum of states of the transition state, which are required for the RRKM part of the calculations,[29] is quite straightforward. This is not the case for gas-phase electron transfer reactions. More recently, Han, Wilbur, and Brauman[30b] have reported also calculations for some electron transfer reactions. While the transition state models used are straightforward and interesting, the systems treated did not include cases where large geometry changes occur.

Because of the complexities of the electron transfer involving η^4-BdFe$(CO)_3$ and its anion and the almost complete lack of detailed structural information on the anion, it appears that a more complete utilization of the kinetic data, Table II, on the basis of kinetic models will not be possible. For the time being one can say only that the present results are completely consistent with a large geometry change as would be expected due to the structures of η^2-BdFe$(CO)_3^{\bullet-}$ and η^4-BdFe$(CO)_3$.

(c) Unimolecular Dissociation of η^2-BdFe$(CO)_3^{\bullet-}$. In competition with the electron transfer reactions described in sections a and b, the η^2-BdFe$(CO)_3^{\bullet-}$ anion also undergoes a unimolecular elimination of CO, reaction 10.

$$\eta^2\text{-BdFe}(CO)_3^{\bullet-} \rightarrow \eta^4\text{-BdFe}(CO)_2^{\bullet-} + CO \qquad (10)$$

It is assumed that recoordination of the loose C=C bond occurs concomitantly with the CO elimination in this reaction. The

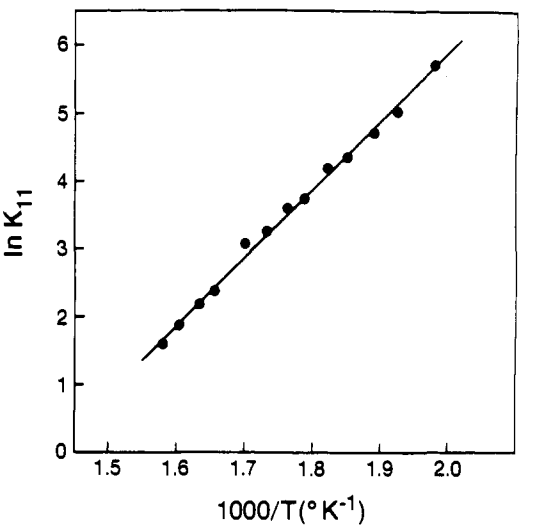

Figure 6. van't Hoff plot of equilibrium constant K_{11} for the equilibrium η^4-BdFe$(CO)_2^{\bullet-}$ + CO = η^2-BdFe$(CO)_3^{\bullet-}$.

η^4-BdFe$(CO)_2^{\bullet-}$ anion is therefore a 17-electron species like η^2-BdFe$(CO)_3^{\bullet-}$ and $Fe(CO)_4^{\bullet-}$. Electron capture by η^4-BdFe-$(CO)_3$ produced η^2-BdFe$(CO)_3^{\bullet-}$ rather than η^4-BdFe$(CO)_2^{\bullet-}$ + CO which implies that a Fe–alkene bond is cleaved more readily than a Fe–CO bond. Therefore, reaction 10 should be endothermic. This was confirmed by the observation that the unimolecular rate constant for reaction 10, k_{10} increases as the reaction temperature is increased.[31-33] From the slope of the Arrhenius plot of ln k_{10} versus $1000/T$ (K) shown in Figure 5, an activation energy of E_{a10} = 19.9 kcal mol^{-1} ($A_{10} = 1.2 \times 10^{13}$ s^{-1}) was determined for reaction 10.

By replacing the methane in the reaction mixtures with neat carbon monoxide, it was possible to measure the equilibrium constant for the clustering equilibrium shown in reaction 11, which

$$CO + \eta^4\text{-BdFe}(CO)_2^{\bullet-} + \eta^2\text{-BdFe}(CO)_3^{\bullet-} \qquad (11)$$

$$K_{10} = \frac{[\eta^2\text{-BdFe}(CO)_3^{\bullet-}]}{[\eta^4\text{-BdFe}(CO)_2^{\bullet-}][CO]}\ (\text{atm}^{-1})$$

is the reverse of reaction 10. From the van't Hoff plot of ln K_{11} versus $1000/T$ (K), shown in Figure 6, it was determined that ΔH°_{11} = −20.0 kcal mol^{-1} and ΔS°_{11} = −28.3 cal K^{-1} mol^{-1}. The near-equivalence of E_{a10} and $-\Delta H^\circ_{11}$ shows that the forward reaction 11 proceeds with a small activation energy and that the activation energy measured for the loss of CO in reaction 10 is actually approximately equal to the endothermicity of the reaction; $-\Delta H^\circ_{10} \approx E_{a10} + RT$ = 20.7 kcal mol^{-1}.

The enthalpy change $-\Delta H^\circ_{11}$, could be formally represented by the difference in formal bond energies, i.e., [CO–Fe(alkene)$(CO)_2^{\bullet-}$] − [(alkene)–Fe(alkene)$(CO)_2^{\bullet-}$] = 20 kcal mol^{-1}, where each (alkene) represents one of the C=C bonds of the butadiene. The 20-kcal mol^{-1} difference in formal bond energies involving the negative ions is found to be close to a corresponding

(28) Sutin, N. *Prog. Inorg. Chem.* **1983**, *30*, 441.
(29) Marcus, R. A.; Sutin, N. *Inorg. Chem.* **1975**, *14*, 213.
(30) (A) Dodd, J. A.; Brauman, J. I. *J. Phys. Chem.* **1986**, *90*, 3559. (b) Han, C. C.; Wilbur, J. L.; Brauman, J. I. *J. Am. Chem. Soc.* **1992**, *114*, 887.

(31) We have made the assumption that reaction 10 is first order and the reverse reaction 11 is second order, so that conventional Arrhenius-type dependence can be assumed for reaction 10. However, under our conditions, reactions like (11) are commonly third order, i.e., third body dependent, and therefore the reverse reaction, i.e., (10) should be second order and then equations from the energy transfer mechanism[32] should apply.[33] Unfortunately, the third body dependence of reaction 10 was not measured. We assume that reaction 10 is first order, because the preexponential factor A_{10} = 10^{13} s^{-1} is so close to values expected[23] for first-order decomposition reactions. When the energy transfer mechanism applies, the E_a obtained with the Arrhenius treatment is found to be smaller than the actual transition state energy $E^{\ddagger}$ by a few kcal/mol, i.e., by the negative "activation energy" of the reverse process which has negative temperature dependence.[33]
(32) Palmer, H. B.; Hornig, D. F. *J. Chem. Phys.* **1957**, *26*, 98. Porter, G. *Discuss. Faraday Soc.* **1962**, *33*, 198. Fowler, R. H.; Guggenheim, E. A. *Statistical Thermodynamics*; Cambridge University Press: Cambridge, England, 1939; p 497.
(33) Durden, D. A.; Kebarle, P.; Good, A. *J. Chem. Phys.* **1969**, *50*, 805.

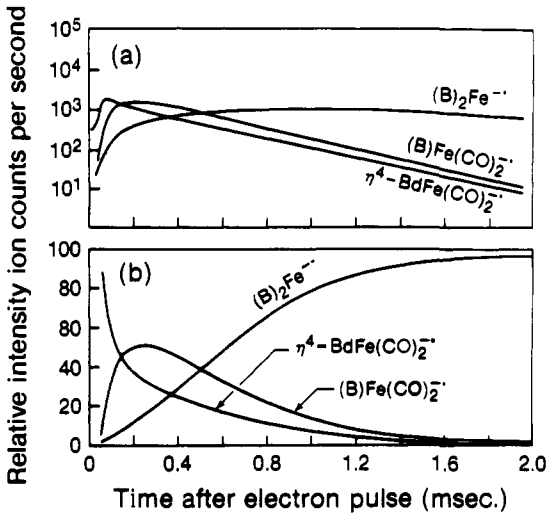

Figure 7. Plots of intensities of significant ions observed with a reaction mixture containing 27 mTorr of η^4-$BdFe(CO)_3$ and 1.5 mTorr of *m*-(CF_3)nitrobenzene in 6 Torr of methane at 150 °C: (a) logarithmic plot of intensities observed; (b) intensities as percent of total. Intensity changes with time indicate the reaction sequence: η-4-$BdFe(CO)_2^{\cdot-} \rightarrow$ = $(B)Fe(CO)_2^{\cdot-} \rightarrow (B)_2Fe^{\cdot-}$, where B = (CF_3)nitrobenzene.

bond energy difference involving the neutral species. Thus, D-[CO–$Fe(CO)_4$] = 41.5 kcal/mol[34] and D[ethylene–$Fe(CO)_4$] = 23.1 kcal mol[24] lead to a difference of 18.4 kcal mol^{-1} for the bonds in the neutral species.

(d) Reactions of η^4-$BdFe(CO)_2^{\cdot-}$. In addition to the ions arising from reactions 4–10, the mass spectra of the reaction mixtures frequently contained other ions such as $(B)Fe(CO)_2^{\cdot-}$ and $(B)_2Fe^{\cdot-}$, where B = nitrobenzene, *m*-fluoronitrobenzene, *m*-(trifluoromethyl)nitrobenzene, *o*-nitrobenzaldehyde, and 3,5-bis(trifluoromethyl)nitrobenzene. The formation of these ions indicates that substituted nitrobenzenes may displace butadiene and CO from the coordination sphere of the iron in the gas phase. From an examination of the time dependence of the various ions in the mass spectra at various concentrations of B and η^4-$BdFe(CO)_3$, it could be established that the precursor for the $(B)Fe(CO)_2^{\cdot-}$ and $(B)_2Fe^{\cdot-}$ ions was η^4-$BdFe(CO)_2^{\cdot-}$. A typical set of ion time profiles is shown in Figure 7. Reactions 12 and 13 are suggested

$$\eta^4\text{-}BdFe(CO)_2^{\cdot-} + B \rightarrow (B)Fe(CO)_2^{\cdot-} + Bd \quad (12)$$

$$(B)Fe(CO)_2^{\cdot-} + B \rightarrow (B)_2FeCO^{\cdot-} + CO \quad (13)$$

as the most probable sources of the $(B)Fe(CO)_2^{\cdot-}$ and $(B)_2Fe^{\cdot-}$ ions. No evidence was found to suggest that η^2-$BdFe(CO)_3^{\cdot-}$ undergoes similar reactions, which is reasonable since, as established in section c, η^2-$BdFe(CO)_3^{\cdot-}$ is 20 kcal mol^{-1} more stable than η^4-$BdFe(CO)_2^{\cdot-}$. Also, no evidence was found to suggest that reactions between $B^{\cdot-}$ and η^4-$BdFe(CO)_3$ were involved in the formation of $(B)Fe(CO)_2^{\cdot-}$ and $(B)_2Fe^{\cdot-}$.

The ions of the form, $(B)_2Fe^{\cdot-}$, in which the butadiene and all of the CO ligand have been replaced by the two substituted nitrobenzene ligands, are particularly interesting. Since d^8 Fe^0 may coordinate only five electron pairs from surrounding ligands as a consequence of the 18-electron rule, but the two B ligands may donate a total of six π-electron pairs, it is probable that the bonding in the two ligands is different. A plausible bonding arrangement is (η^4-B)Fe(η^6-$B^{\cdot-}$), where one of the aromatic ligands distorts and bonds as a tetrahapto species in which only two of its π-electron pairs are involved in bonding with the iron atom, and the second ligand acts as a conventional hexahapto arene donor. As the iron atom would be unable to accommodate the negative charge due to its full (i.e., 18-electron) valence shell, the negative charge must reside in the π^* LUMO of the η^6 aromatic ligand. Analogous molecules of the form, (η^4-B)M(η^6-B), where M is a group VIIIa metal and B is a substituted benzene, have been prepared and characterized.[5] A 17-electron structure for $(B)_2Fe^{\cdot-}$ is conceivable, where both of ligands bond as tetrahapto species and the negative charge is located on the iron atom, i.e., (η^4-$B)_2Fe^{\cdot-}$, but this structure would involve disruption of the aromatic system in both ligands and is therefore likely to be less stable than (η^4-B)Fe(η^6-$B^{\cdot-}$). The $(B)Fe(CO)_2^{\cdot-}$ ions are likely to be of the form, $(CO)_2Fe(\eta^6\text{-}B^{\cdot-})$, since this arrangement would allow the iron to achieve a full valence shell while retaining a low-lying LUMO on B to accommodate the negative charge.

Low intensity ions were identified in the mass spectra arising from unimolecular loss of an oxygen atom from the nitro group of the substituted nitrobenzenes. This is a frequently encountered loss from substituted nitrobenzene anions (i.e., $B^{\cdot-}$) under PHPMS conditions[35] and probably occurs from ions such as $(B)Fe(CO)_2^{\cdot-}$ and $(B)_2Fe^{\cdot-}$ also. The mass spectra also typically contained an ion of the form, $(B)Fe^{\cdot-}$, but the origin of this ion was not identified.

In previous studies[36] of the reactions of anionic nucleophiles with $Fe(CO)_5$ in the gas phase, it was noted that addition of the nucleophile to one of the CO molecules to form a coordinated acyl anion, reaction 14, was a major reaction pathway for many anions.

$$Fe(CO)_5 + X^- \rightarrow Fe(CO)_4CXO^- \rightarrow XFe(CO)_{5-n}^- + nCO \quad (14)$$

Presumably, analogous reactions may occur with η^4-$BdFe(CO)_3$ involving nucleophile addition to CO or Bd, but ions arising from such processes under PHPMS conditions were not identified in the present work. With the exception of electron transfer reactions, the $B^{\cdot-}$ anions were found to be unreactive toward η^4-$BdFe(CO)_3$. These differences are probably due to the marked reactivity differences to be expected between the even-electron X^- anions studied previously and the odd-electron $B^{\cdot-}$ anions generated in this study. The reactive X^- ions were generally "hard" species such as halides, hydroxide, amide, etc., in which the negative charge was localized on one atom, and which are likely to be much more nucleophilic than substituted nitrobenzene anions in which the negative charge is completely delocalized.

No evidence was found to indicate that dimerization reactions of η^2-$BdFe(CO)_3^{\cdot-}$ or η^4-$BdFe(CO)_3$ with η^4-$BdFe(CO)_3$ were prevalent under the PHPMS experimental conditions.

(34) Lewis, K. E.; Golden, D. M.; Smith, G. P. *J. Am. Chem. Soc.* **1984**, *106*, 3905.

(35) Dillow, G. W.; Kebarle, P. Unpublished results.

(36) (a) Lane, K. R.; Sallans, L.; Squires, R. R. *J. Am. Chem. Soc.* **1985**, *107*, 5369. (b) Lane, K. R.; Sallans, L.; Squires, R. R. *J. Am. Chem. Soc.* **1986**, *108*, 4368.